

# VALIDATION OF 3D PULSE SEQUENCE FOR LARGE VOLUME ACOUSTIC RADIATION FORCE IMPULSE IMAGING

Joshua de Bever<sup>1</sup>, Nick Todd<sup>2</sup>, Allison Payne<sup>2</sup>, Mahamadou Diakite<sup>2</sup>, John Hollerbach<sup>1</sup>, and Dennis Parker<sup>2</sup>

<sup>1</sup>School of Computing, University of Utah, Salt Lake City, Utah, United States, <sup>2</sup>Utah Center for Advanced Imaging Research, University of Utah, Salt Lake City, Utah, United States

**Introduction** Previous methods for Acoustic Radiation Force Impulse imaging (ARFI) have demonstrated the utility of visualizing the ultrasound (US) pressure pattern [1–3]. The pulse sequence presented here extends previous work by leveraging the improved SNR of 3D imaging to provide large coverage volumetric ARFI imaging. Large volume 3D ARFI imaging would be especially beneficial for easily and safely verifying targeting accuracy before an MR guided HIFU treatment.

**Methods** A 3D Spin-Echo segmented EPI pulse sequence was modified to include two pairs of bipolar motion encoding (ME) gradients (Figure 1). An optical trigger is output on the rising edge (center) of each bipolar ME gradient lobe which synchronizes the firing of an ultrasound burst. This sequence was run on a Siemens 3T Trio MRI scanner with an ultrasound generator system (Image Guided Therapy, Bordeaux, France) and 256-element phased-array transducer (Imasonic, Besancon, France). Circuitry to convert the optical trigger pulses from the MRI to TTL pulses for the US generator was designed and built by the authors. This custom device includes fault detection to ensure that the US is automatically turned off if the MRI's 'off' trigger is lost.

Two experiments were performed to test the 3D ARFI sequence in a tissue-mimicking phantom (ATS Laboratories) positioned approximately 11cm above the phased-array transducer: (1) with the US focal spot offset by (0,0,15)mm from its geometric focus, and (2) with the US focal spot offset by (5,5,15)mm. For each experiment, one static 3D image was acquired without US bursts and a second dynamic 3D image with US bursts (127 acoustic W, 24.4 ms/TR, 4.8% duty cycle) synchronized with the ME gradient. The ARFI phase difference was obtained as the phase increment between the two measurements:  $\text{angle}(z_2 \times z_1^*)$ . MR-ARFI acquisition parameters: TR/TE = 250/56ms, 16 slices with resolution = 2x2x2mm and FOV = 128x256x32mm, 25% slice oversampling, EPI factor = 5, Flip Angle = 70°, Bandwidth = 752 Hz/px, ME-Amp = 25mT/m, ME-Dur = 40ms. Total acquisition time for both measurements = 2.5min.

To validate the ARFI maps a second set of experiments measured temperature over the same volume using a 3D segmented EPI Proton Resonance Frequency (PRF) thermometry sequence. A single 20 sec US sonication at 12.5 acoustic watts was delivered to each focal spot location tested in the ARFI experiments. The PRF acquisition parameters were: TR/TE = 25/10 ms, 16 slices with resolution = 2x2x2mm and FOV = 128x256x32mm, 25% slice oversampling, EPI = 5, Flip Angle = 20°, bandwidth = 710 Hz/px, Acquisition Time = 6.5sec/meas. The 3D ARFI and PRF maps were zero-fill-interpolated to 1x1x1mm voxel spacing, and then analyzed for corresponding peak positions.

**Results** Figure 2a and 2b show sagittal and coronal slices through the 3-D ARFI volume depicting the US beam at locations of maximum ARFI phase difference when the focal spot was steered to (0,0,15)mm. The corresponding temperature map in figure 2c show qualitatively that the location of peak temperature corresponds with the location of peak ARFI phase difference. Figure 3a and 3b show the ARFI peak when the US focal spot is steered 5mm in *x* and *y*. Figure 4a demonstrates quantitatively that the peak ARFI displacement shifts the expected 5mm in the *x*-direction, and thus the measured ARFI signal successfully tracks the focal zone offset. An independent validation of the previous result is shown in figure 4b where the location of peak temperature moves the same 5mm distance. The drop in ARFI phase difference in figure 4a demonstrates that 3D ARFI successfully captures the expected reduced pressure at the focus due to reduced constructive beam interference as steered distance increases. The temperatures shown in figure 4b further demonstrate this phenomenon. The utility of 3D ARFI's volumetric coverage is also demonstrated in figure 2a and 3a where the expected beam tilting associated with phased-array steering is captured in the 3D ARFI maps.

**Conclusion & Future Work** The 3D ARFI sequence developed here successfully tracked the movement, amplitude reduction, and tilting of the focal spot and correlated with 3D temperature maps. Several easy to implement optimizations exist that would reduce the acquisition time and US duty cycle. This sequence could be used before an MR guided HIFU treatment to safely verify targeting accuracy without causing significant heating, and by comparing pre/post treatment 3D ARFI maps, it might be possible verify treatment efficacy by identifying changes in tissue mechanical properties. This 3D ARFI sequence covers a significantly larger volume than 2D approaches providing precise localization in all three dimensions, thus increasing the chance the peak pressure will be accurately measured. This is especially important for *in vivo* applications where tissue inhomogeneities can cause the focal spot location to deviate significantly from the simple geometric prediction.

**Literature Cited** [1] N. McDannold, "Magnetic resonance acoustic radiation force imaging," *Med. Phys.*, vol. 35, p. 3748, 2008. [2] J. Chen, "Optimization of encoding gradients for MR-ARFI," *MRM*, vol. 63, pp. 1050-1058, Apr. 2010. [3] E. A. Kaye, "Rapid MR-ARFI method for focal spot localization during focused ultrasound therapy," *MRM*, vol. 65, pp. 738-743, Mar. 2011.

**Acknowledgements** This work is supported by the Mark H. Huntsman Endowed chair, NIH grants R01 CA87785 and R01 CA134599, The Ben B. and Iris M. Margolis Foundation, NSF IGERT Award# 0654414, and the Focused Ultrasound Surgery Foundation.

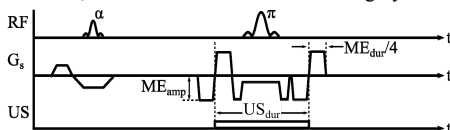


**Figure 1** Schematic of 3D MR-ARFI pulse sequence and relevant parameters.

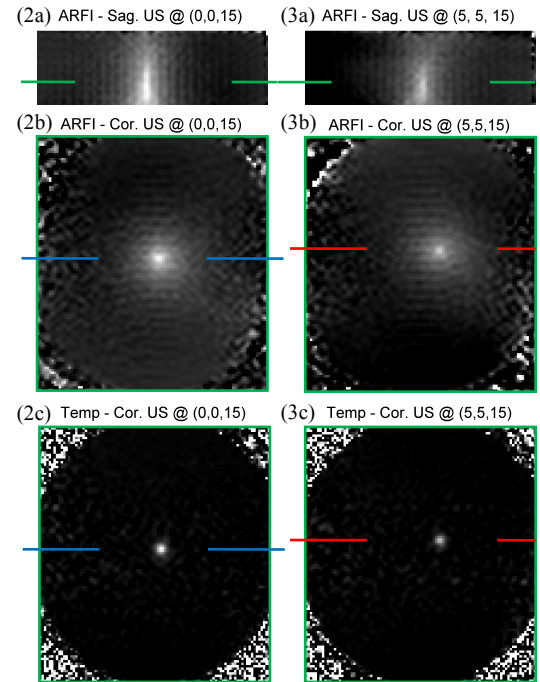


**Figure 2** (a) Sagittal slice through peak of 3D ARFI map when US fired at (0,0,15) (b) coronal slice through peak ARFI signal, ARFI signal along blue line plotted in figure 4a, (c) coronal slice of 3D temperature map; same slice location as (2b), temperatures along blue line plotted in figure 4b.

**Figure 3** (a) Sagittal slice through peak of 3D ARFI map when US fired at (5,5,15) (b) coronal slice through peak ARFI signal, ARFI signal along red line plotted in figure 4a, (c) coronal slice of 3D temperature map; same slice location as (3b), temperatures along red line plotted in figure 4b.

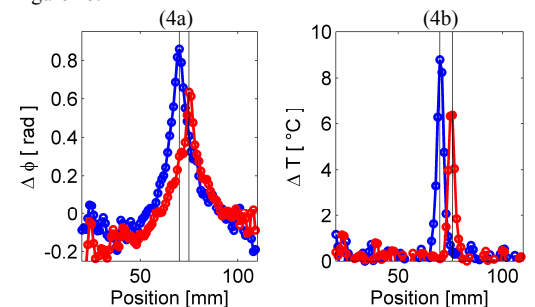


**Figure 4** (a) Blue: 3D ARFI signal along blue line in fig. 2b, US @ (0,0,15). Red: 3D ARFI signal along red line in fig. 3b, US @ (5,5,15). (b) Blue: 3D temperatures along blue line in fig. 2c, US @ (0,0,15). Red: 3D temperatures along red line in fig. 3c, US @ (5,5,15).